Hindawi Publishing Corporation
Journal of Biomedicine and Biotechnology
Volume 2010, Article ID 518743, 14 pages
doi:10.1155/2010/518743

Research Article

Elementary Mode Analysis for the Rational Design of Efficient Succinate Conversion from Glycerol by *Escherichia coli*

Zhen Chen,[1,2] Hongjuan Liu,[1] Jianan Zhang,[1] and Dehua Liu[2]

[1] *Institute of Nuclear and New Energy Technology, Tsinghua University, Beijing 100084, China*
[2] *Department of Chemical Engineering, Institute of Applied Chemistry, Tsinghua University, Beijing 100084, China*

Correspondence should be addressed to Hongjuan Liu, liuhongjuan@tsinghua.edu.cn and Jianan Zhang, zhangja@tsinghua.edu.cn

Received 2 December 2009; Revised 20 May 2010; Accepted 7 July 2010

Academic Editor: Jennifer Reed

By integrating the restriction of oxygen and redox sensing/regulatory system, elementary mode analysis was used to predict the metabolic potential of glycerol for succinate production by *E. coli* under either anaerobic or aerobic conditions. It was found that although the theoretical maximum succinate yields under both anaerobic and aerobic conditions are 1.0 mol/mol glycerol, the aerobic condition was considered to be more favorable for succinate production. Although increase of the oxygen concentration would reduce the succinate yield, the calculation suggests that controlling the molar fraction of oxygen to be under 0.65 mol/mol would be beneficial for increasing the succinate productivity. Based on the elementary mode analysis, the rational genetic modification strategies for efficient succinate production under aerobic and anaerobic conditions were obtained, respectively. Overexpressing the phosphoenolpyruvate carboxylase or heterogonous pyruvate carboxylase is considered to be the most efficient strategy to increase the succinate yield.

1. Introduction

Glycerol has become an abundant and inexpensive carbon source due to its generation as an inevitable byproduct of biodiesel production. Over the past few years, the price of crude glycerol has decreased 10-fold due to the tremendous growth of the biodiesel industry [1]. Much effort has been paid for the development of processes to convert crude glycerol into higher-value products to maximize the full economic potential of biodiesel process. For example, the transformation of glycerol into 1,3-propanediol has been extensively studied in the past few years [2–4].

Several recent studies also tried to utilize glycerol as a carbon source for the transformation of other valued products such as ethanol [5] and amino acids [6]. Succinate is traditionally produced from sugars and suffers the limitation due to the availability of reducing equivalents. Compared with glucose, glycerol has a higher reduced state and also several microorganisms such as *E. coli* can transform glycerol into succinate [7]. So, the byproduct glycerol is a potential substrate for the succinate production. Despite few attempts in the past, no industrially competitive organisms can effectively produce succinate from glycerol so far. In the light of the new powerful tools of metabolic engineering, the quest for targeted development of strains that can effectively utilize glycerol for succinate production is strongly revived. *E. coli* is one of the most promising organisms since it can directly utilize glycerol and it has been traditionally developed for succinate production [8–10].

The dissimilation of glycerol in *E. coli* is catalyzed by proteins encoded by *glp* regulon under aerobic conditions. Glycerol is first phosphorylated into glycerol 3-phophate (G3P) by ATP-dependent glycerol kinase encoded by *glpK* gene, and then glycerol 3-phophate is converted into dihydroxyacetone phosphate (DHAP) by aerobic G3P dehydrogenase encoded by *glpD* gene (Figure 1) [11, 12].

Although the aerobic utilization of glycerol by *E. coli* has been known for a long time, the fermentative pathway of glycerol has just been clarified recently [13, 14]. It has been suggested that the feasibility of fermenting glycerol into fuels and other reduced chemicals is through the inducing of its native 1,2-propanediol fermentative pathway without

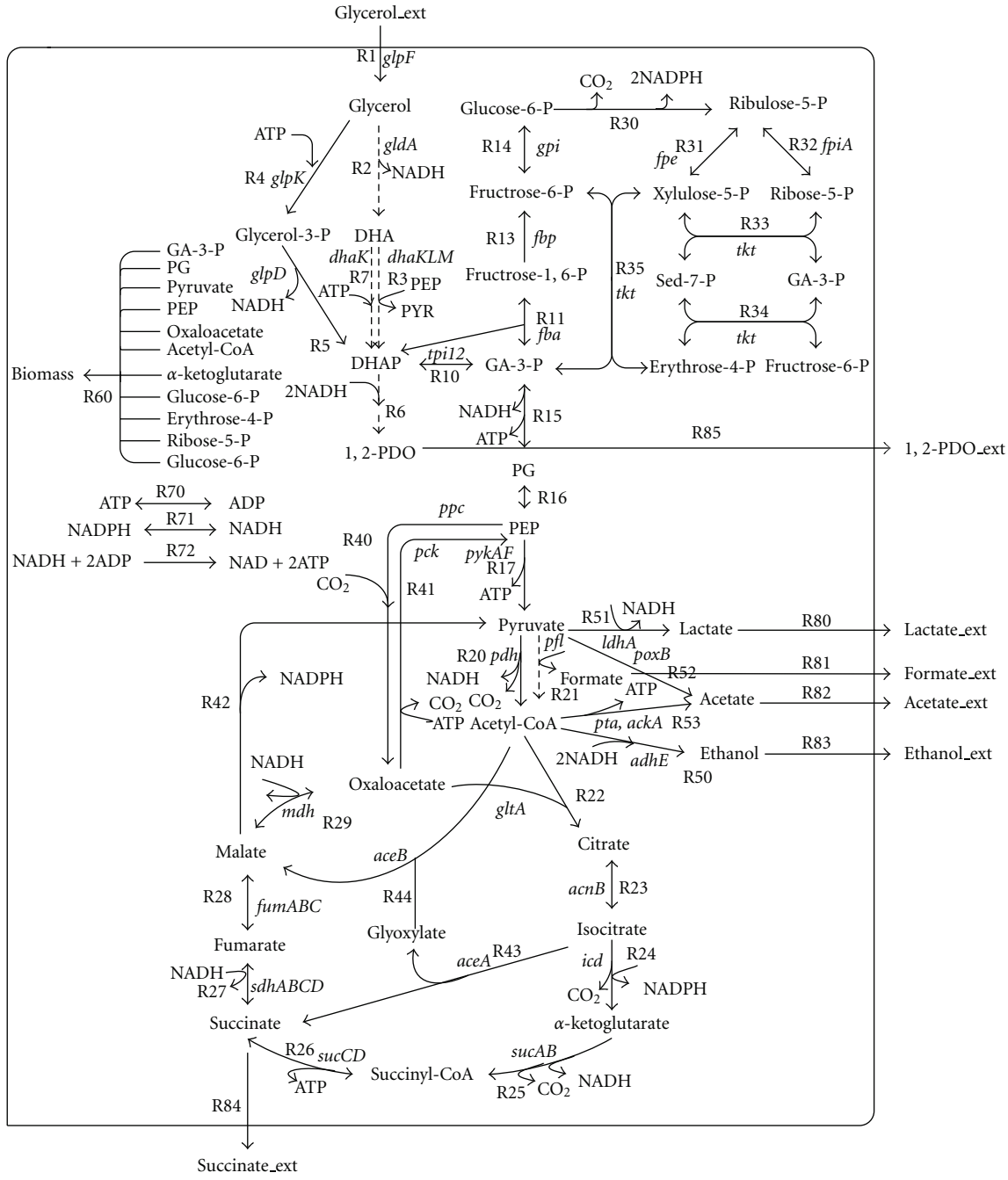

Figure 1: Central metabolic network of glycerol in wildtype *E. coli*. The dashed arrows represent the particular pathways in anaerobic conditions. Reversible reactions are represented by a double-headed arrow. Key genes associated with the pathway are included.

using external electron acceptors. In this pathway, glycerol is converted to dihydroxyacetone (DHA) by NAD^+-linked glycerol dehydrogenase (GDH), and the DHA is phosphorylated to DHAP via the ATP-dependent or phosphoenolpyruvate (PEP)-dependent DHA kinase (DHAK). DHAP is then reduced into 1,2-propanediol or enter glycolysis [15].

Since *E. coli* can utilize glycerol in both aerobic and anaerobic conditions, it is necessary to analyze the potential and the feasibility of engineering *E. coli* for the succinate production in either condition. A careful metabolic pathway analysis is very helpful in such kind of estimation and rational strain development. Elementary mode analysis is one of the most powerful tools for metabolic pathway analysis using for the metabolic properties study of cellular systems [16–18]. Elementary mode analysis allows the calculation of a solution space that contains all possible steady-state flux distributions of a network. The stoichiometry of the metabolic network, including carbon as well as cofactor requirements, is fully considered in elementary mode analysis. On the other hand, it also allows determining the overall capacity, that is,

theoretical maximum yield, of a cellular system and studying the effects of any genetic modification. Based on such studies, rational design can be obtained for the efficient production and genetic modification. Moreover, knowledge of the theoretical maximum yield allows estimating the potential economic efficiency of a process. Recently, elementary mode analysis has been used for genome scale metabolic studies dealing with, for example, the rational design of methionine production in *E. coli* and *C. glutamicum* [19], the production of polyhydroxybutanoate in yeast [20], and growth-related aspects in *Saccharomyces cerevisiae* [21, 22] and *E. coli* [23, 24].

In this work, the elementary mode analysis was carried out for succinate production by comparing the metabolic networks of *E. coli* in anaerobic and aerobic conditions. The pathways involved in the flux scenario representing optimal succinate production were investigated and the effect of oxygen level on succinate production and biomass was also discussed. Furthermore, the rational design for the genetic modification of the *E. coli* to enhance the succinate production was developed. This work is considered useful for the further strain improvement and metabolic regulation in the succinate production by *E. coli* with glycerol as the substrate.

2. Materials and Methods

2.1. Metabolic Reaction Network. The glycerol metabolic network of *E. coli* was constructed (Figure 1) based on KEGG database (http://www.genome.jp/kegg/metabolism.html) as well as biochemical and physiological literatures [13, 14, 25]. It includes glycerol dissimilation pathways, glycolysis pathway (EMP), pentose phosphate pathway (PPP), tricarboxylic acid (TCA) cycle, biosynthesis pathway, anaplerosis, and respiratory chain. The metabolic network was depicted in Figure 1. For the interconversion of NADH and NADPH, a cytosolic transhydrogenase transferring protons from NADPH to NAD^+ and a membrane-bound transhydrogenase reducing $NADP^+$ by oxidation of NADH were implemented [26]. For ATP production in the respiratory chain, a P/O ratio of 2 for NADH was assumed [27].The precursor demand for biomass formation was calculated according to the literature [28]. The biomass term is represents as Cmol basis ($CN_{0.24}S_{0.008}$). The cell physiology of *E. coli* is strongly affected by oxygen from different levels such as the transcriptional regulatory which cannot be represented simply in the metabolic network. For example, one component fumarate and nitrate reduction (FNR) protein is aerobic/anaerobic response regulator [25]. FNR appears to sense oxygen directly through a redox-sensitive iron-sulphur cluster in the protein and is active only during anaerobic growth. The two iron-sulphur ($[4Fe–4S]^{2+}$) clusters in the dimeric FNR protein are converted to two $[2Fe–2S]^{2+}$ clusters upon exposure to stoichiometric levels of oxygen. Active FNR protein activates and represses target genes in response to anaerobiosis. It acts as a positive regulator of genes expressed under anaerobic fermentative conditions such as aspartase, formate dehydroganases, fumarate reductase, and pyruvate formate lyase. To account for the effects of FNR regulator and other experimental discovery, the following constraints are used to discriminate the metabolic networks under aerobic and anaerobic network.

For the anaerobic model, glycerol is assumed to be dissimilated into DHA by NAD^+-dependent glycerol dehydrogenase and then DHA is phosphorylated into DHAP by ATP-dependent or PEP-dependent DHA kinase [13, 14]. The pathway from DHAP to 1,2-propanediol is considered to be active under anaerobic condition [13]. The pyruvate dehydrogenase complex is inactive under anaerobic condition and thus pyruvate-formate lyase was the only active enzyme that catalyzes the transformation of pyruvate into acetyl-CoA [29]. The TCA cycle is broken at the alpha-ketoglutarate dehydrogenase step and the respiratory chain is assumed to be inactive [30]. The detailed description of the model is listed in Appendices A.1 and A.2.

For the aerobic model, glycerol is firstly phosphorylated into G3P by ATP-dependent glycerol kinase and then G3P is transferred into DHAP by NAD^+-dependent G3P dehydrogenase [11, 12]. The 1, 2-propanediol pathway is assumed to be inactive. Pyruvate oxidase is active under aerobic condition which will transfer pyruvate into acetate. The detailed description of the model is listed in Appendices A.1 and A.3.

2.2. Computational Methods. In the present work, the elementary mode analysis was carried out for studying the aerobic and anaerobic metabolism of glycerol in *E. coli* by using METATOOL 5.1 [31]. The script files and compiled shared library of METATOOL 5.1 can be downloaded from the METATOOL website (http://pinguin.biologie.uni-jena.de/bioinformatik/networks/metatool/metatool5.1/metatool5.1.html). The mathematical details of the algorithm were described elsewhere [32]. Metabolic pathway analysis resulted in tens to hundreds of elementary flux modes for each situation investigated. For each of these flux modes, the fluxes were calculated as relative molar values normalized to the glycerol uptake rate and were expressed as mol/mol (glycerol).

3. Results and Discussion

3.1. Elementary Mode Analysis of Glycerol Metabolism under Anaerobic Condition. Under anaerobic condition, the metabolic network model got 55 elementary flux modes. The relationship between the yields of products and biomass was shown in Figure 2. The maximum molar yield of biomass under anaerobic condition is 0.187 mol/mol in which the respective yields of 1,2-propanediol, ethanol, and formate were 0.248 mol/mol, 0.495 mol/mol, and 0.57 mol/mol and no succinate, acetate, and lactate were produced. It was found that the cell growth was always associated with the production of 1,2-propandediol, ethanol, and formate. Therefore, the production of 1,2-propanediol, ethanol, and formate was necessary for the biomass synthesis during the glycerol metabolism. The biomass synthesis process consumes ATP and produces reducing equivalents (NADH). Both ATP

Table 1: Reactions and enzymes involved in Figure 1.

Reactions	Genes	Enzymes	Aerobic/anaerobic specificity	References
R1	*glpF*	glycerol facilitator		[1]
R2	*gldA*	Glycerol dehydrogenase II	anaerobic	[2]
R3	*dhaKLM*	PTS-dependent Dihydroxyacetone kinase	anaerobic	[2]
R4	*glpK*	glycerol kinase	aerobic	[1]
R5	*glpD*	Glycerol-3-phosphate dehydrogenase	aerobic	[1]
R6		sets of reactions	anaerobic	[2]
R7	*dhaK*	ATP-dependent Dihydroxyacetone kinase		[2]
R10	*tpi12*	Triose-phosphate isomerase		KEGG
R11	*fba*	Fructose-bisphosphate aldolase		KEGG
R13	*fbp*	Fructose-bisphosphatase		KEGG
R14	*gpi*	Glucose-6-phosphate isomerase		KEGG
R15		sets of reactions		KEGG
R16		sets of reactions		KEGG
R17	*pykAF*	Pyruvate kinase		KEGG
R20	*pdh*	Pyruvate dehydrogenase	aerobic	[3]
R21	*pfl*	Pyruvate formate-lyase	anaerobic	[4]
R22	*gltA*	Citrate synthase		KEGG
R23	*acnB*	Aconitate hydratase		KEGG
R24	*icd*	Isocitrate dehydrogenase		KEGG
R25	*sucAB*	Oxoglutarate dehydrogenase	aerobic	[5]
R26	*sucCD*	Succinate-CoA ligase	aerobic	[5]
R27	*sdhABCD*	Succinate dehydrogenase		KEGG
R28	*fumABC*	Fumarate hydratase		KEGG
R29	*mdh*	Malate dehydrogenase		KEGG
R30		sets of reactions		KEGG
R31	*rpe*	Ribulose-phosphate 3-epimerase		KEGG
R32	*rpiA*	Ribose-5-phosphate isomerase		KEGG
R33	*tkt*	Transketolase		KEGG
R34	*tkt*	Transaldolase		KEGG
R35	*tkt*	Transketolase		KEGG
R40	*ppc*	PEP carboxylase		KEGG
R41	*pck*	PEP carboxykinase		KEGG
R42	*malE*	malic enzyme		KEGG
R43	*aceA*	Isocitrate lyase		KEGG
R44	*aceB*	Malate synthase		KEGG
R50	*adhE*	Aldehyde dehydrogenase		KEGG
R51	*ldhA*	Lactate dehydrogenase		KEGG
R52	*poxB*	pyruvate oxidase	aerobic	[6]
R53	*pta,ackA*	Phosphate acetyltransferase, Acetate kinase		KEGG
R60		Biomass formation		[7]
R70		ATP-hydrolysis		[7]
R71		Transhydrogenase		[7]
R72		respiratory chain 1	aerobic	[7]
R80		Membrane transport reaction		
R81		Membrane transport reaction		
R82		Membrane transport reaction		
R83		Membrane transport reaction		
R84		Membrane transport reaction		
R85		Membrane transport reaction		

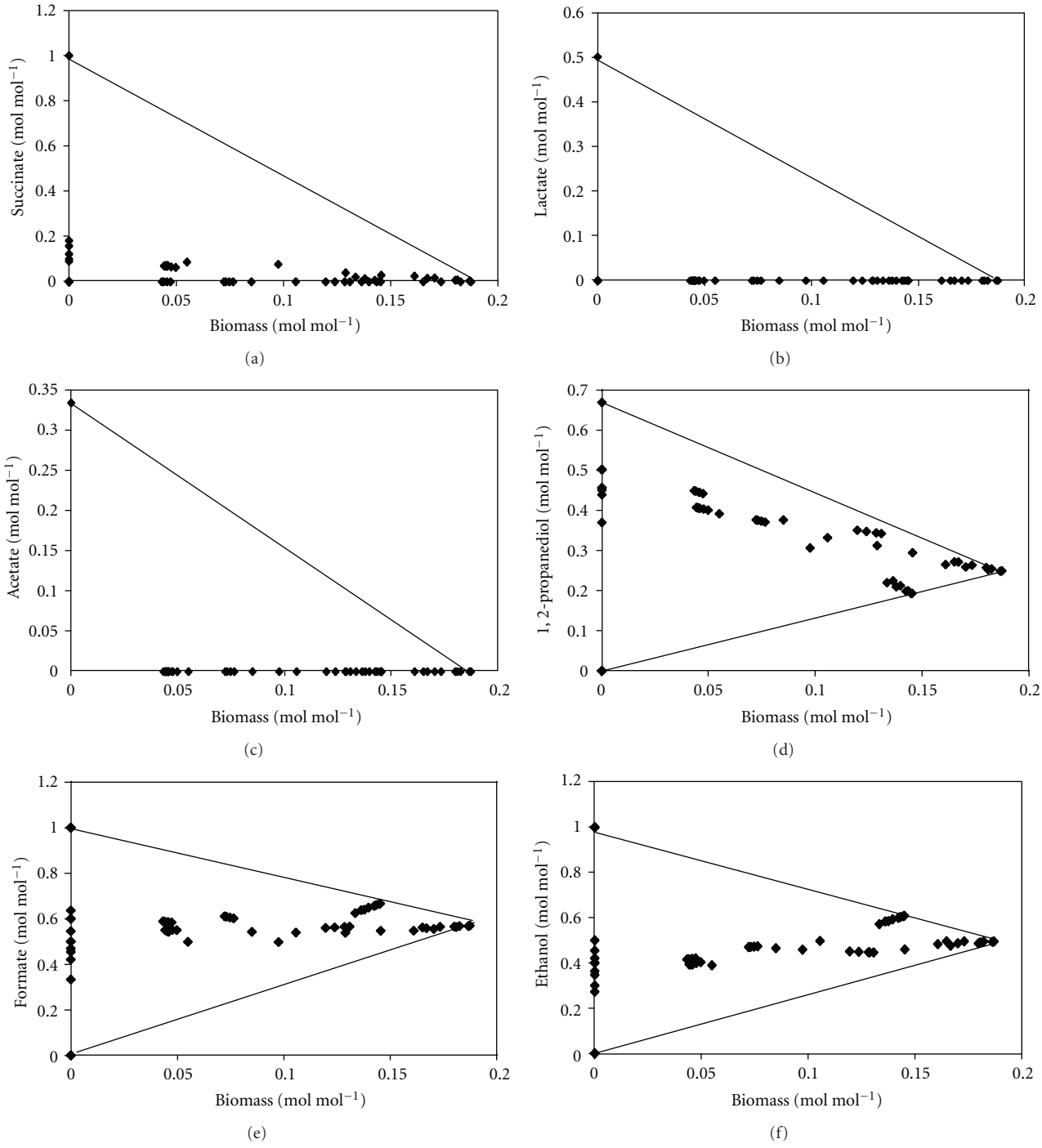

Figure 2: Relationship between the yields of biomass and byproducts for the obtained elementary modes of *E. coli* under anaerobic conditions. (a) Succinate, (b) Lactate, (c) Acetate, (d) 1,2-Propanediol, (e) Formate, and (f) Ethanol. The enclosed regions represent the possible solution space. The fluxes were normalized by glycerol uptake rate and expressed as mol/mol (glycerol).

and NAD need to be regenerated through the production of other byproducts (the biomass synthesis equation in Appendix A.2). For the glycerol metabolism in anaerobic condition, only the glycerol to 1,2-propanediol pathway can consume extra NADH (see (1)) and thus provide the mean to consume the reducing equivalents generated during the synthesis of biomass. The conversion of glycerol to ethanol and formate (see (2)), a redox-balanced pathway, fulfills energy requirements by generating ATP via substrate-level phosphorylation (Appendix A.4). The calculation results were consistent with the experiment observation that 1,2-propanediol and ethanol were growth-associated products

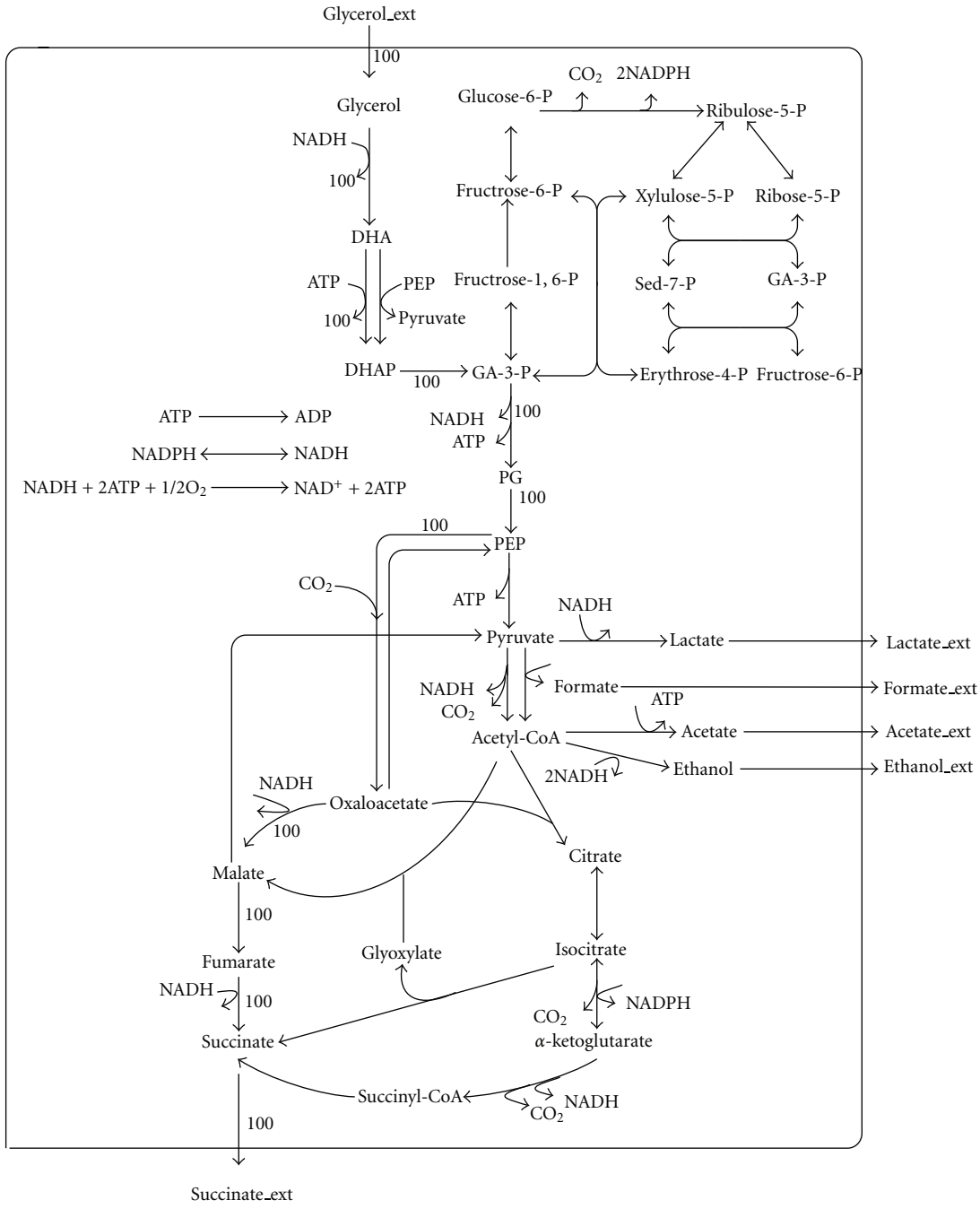

Figure 3: The optimum flux distribution of glycerol metabolism for succinate production in *E. coli* under anaerobic conditions when only ATP-dependent DHA kinase plays a function.

[13, 14]

$$\text{glycerol} + \text{NADH} \longrightarrow 1,2\text{-propanediol} + \text{NAD}, \quad (1)$$

$$\text{glycerol} + \text{ADP} \longrightarrow \text{ethanol} + \text{formate} + \text{ATP}. \quad (2)$$

The maximum succinate yield under anaerobic condition is 1.0 mol/mol when CO_2 or carbonate salts are added as cosubstrates and the optimal flux distribution for succinate production was shown in Figure 3. In this case, there was no production of biomass and other byproducts. The key points for this mode were that the phosphorylation of DHA was only catalyzed by ATP-dependent DHA kinase and PEP was totally carboxylated into oxaloacetate by PEP carboxylase and the latter was further transferred into succinate. This required a very high activity of ATP-dependent DHA kinase and PEP carboxylase. However, it was reported that the PEP-dependent DHA kinase plays the main role in *E. coli* which dramatically reduced the yield of succinate. With single PEP-dependent DHA kinase function, there will be no succinate production [14]. Thus the PEP-dependent DHA kinase is

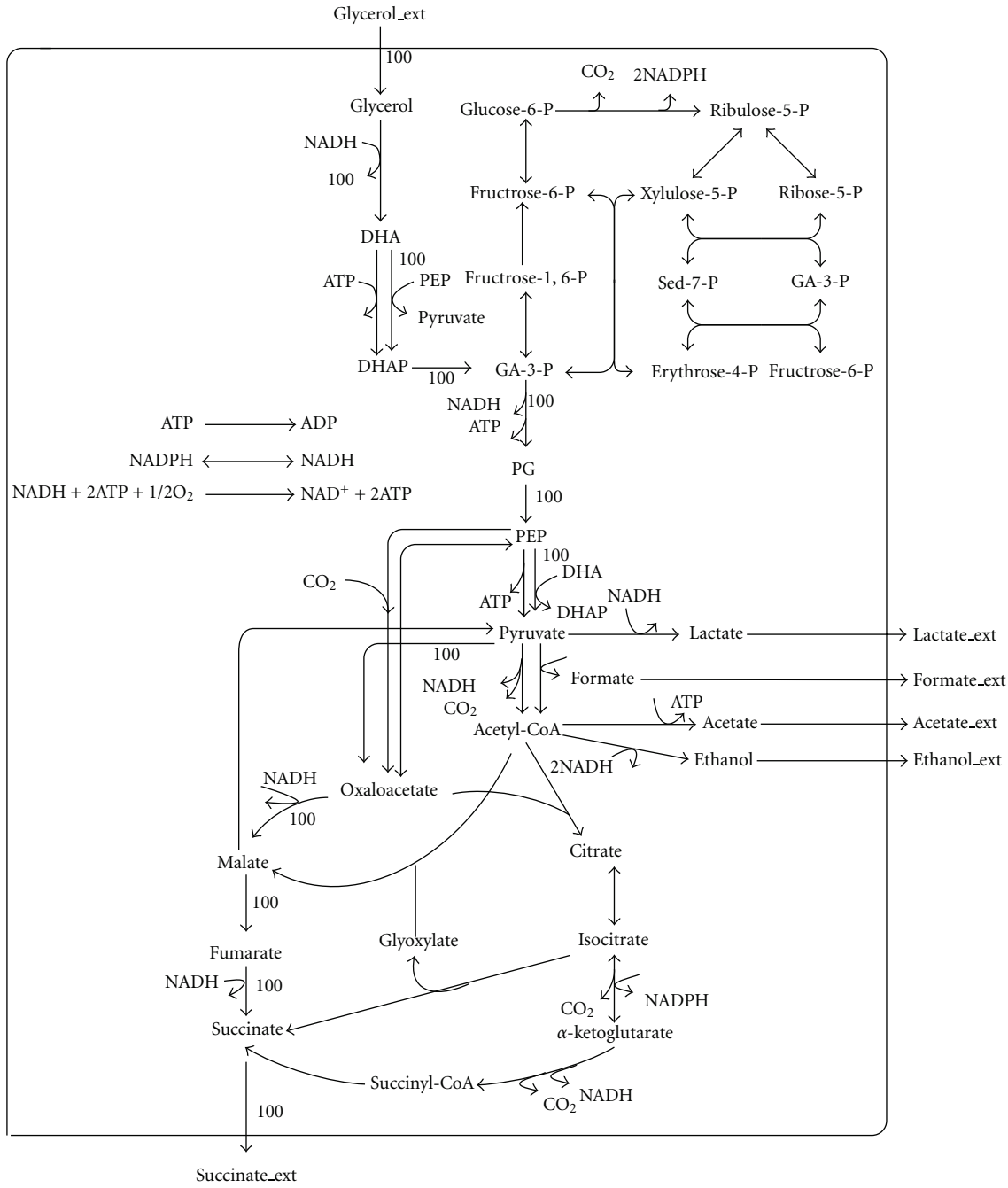

Figure 4: The alternative optimum flux distribution of glycerol metabolism for succinate production in *E. coli* under anaerobic conditions when only PEP-dependent DHA kinase plays a function and heterogeneous PEP carboxylase (pyc) are introduced and overexpressed in *E. coli*.

the bottleneck of succinate production under anaerobic condition.

3.2. Element Ary Mode Analysis of Glycerol Metabolism under Aerobic Condition. The aerobic metabolic network model got 259 elementary flux modes. The relationship between the yields of products and biomass was shown in Figure 5. It was indicated that the flux distribution modes under aerobic condition were completely different from that of anaerobic condition. The maximum molar yield of biomass under aerobic condition was 0.725 mol/mol in which only CO_2 was produced. The results suggested that aerobic condition was more favorable for biomass formation and the most effective way for biomass formation was through the TCA cycle. The cell growth process was no longer associated with the production of 1,2-propanedio, formate, and ethanol. Comparing with the anaerobic condition, the succinate production modes were more diversely distributed throughout

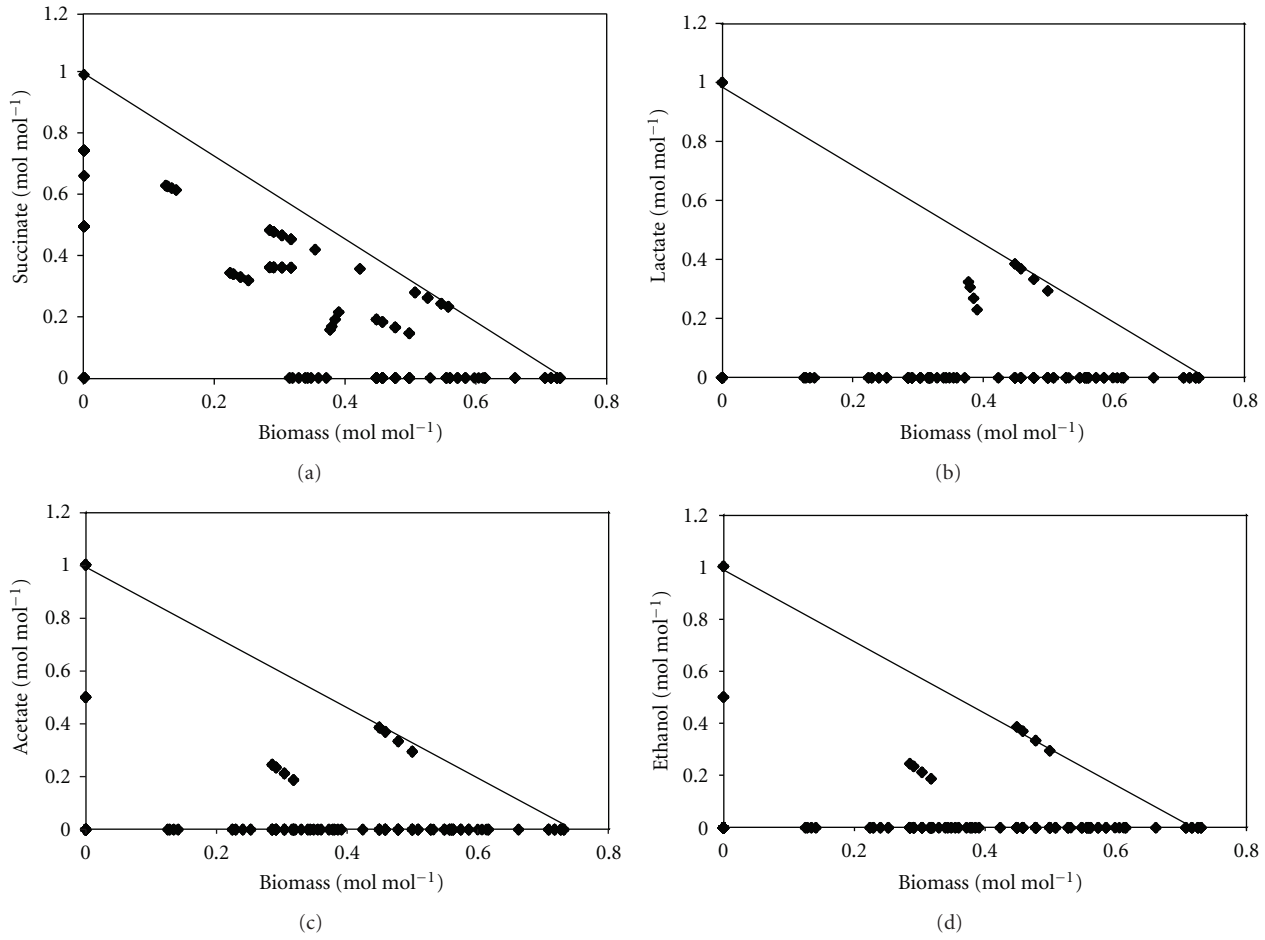

Figure 5: Relationship between the yields of biomass and byproducts for the obtained elementary modes of *E. coli* under aerobic conditions. (a) Succinate, (b) Lactate, (c) Acetate, and (d) Ethanol. The enclosed regions represent the possible solution space. The fluxes were normalized by glycerol uptake rate and expressed as mol/mol (glycerol).

Table 2: Degree of reduction of considered substrates and products.

Glycerol	14
O_2	−4
CO_2	0
Succinate	14
Ethanol	12
Lactate	12
Formate	2
1,2-propanediol	16
Acetate	8

the feasible solution space, and the corresponding yield of succinate at the same biomass yield was higher which indicated that the high potential of succinate production is associated with the cell growth by metabolic modification under aerobic condition.

The maximum succinate yield under aerobic condition (an aerobic mode suggests oxygen consumption) is also 1.0 mol/mol which requires the CO_2 or carbonate salts to be added as cosubstrates, and the optimal flux distribution for succinate production was shown in Figure 6. The optimal flux distribution modes were quite similar for the aerobic and anaerobic conditions. The key point for obtaining high succinate yield was considered as that PEP was totally carboxylated into oxaloacetate by PEP carboxylase and the latter was further transferred into succinate. This required a very high activity of PEP carboxylase.

The network robustness and its sensitivity to perturbation were critical to the optimal metabolic pathway. The sensitivity of succinate yield to the flux ratios at the key branch nodes PEP and acetyl-CoA was considered in this work. PEP was consumed in reactions R40 and R17 which are catalyzed by PEP carboxylase and Pyruvate kinase, respectively; the flux ratio was denoted as

$$\mathrm{R}(40, 17) = \frac{\mathrm{R40}}{(\mathrm{R40} + \mathrm{R17})}. \quad (3)$$

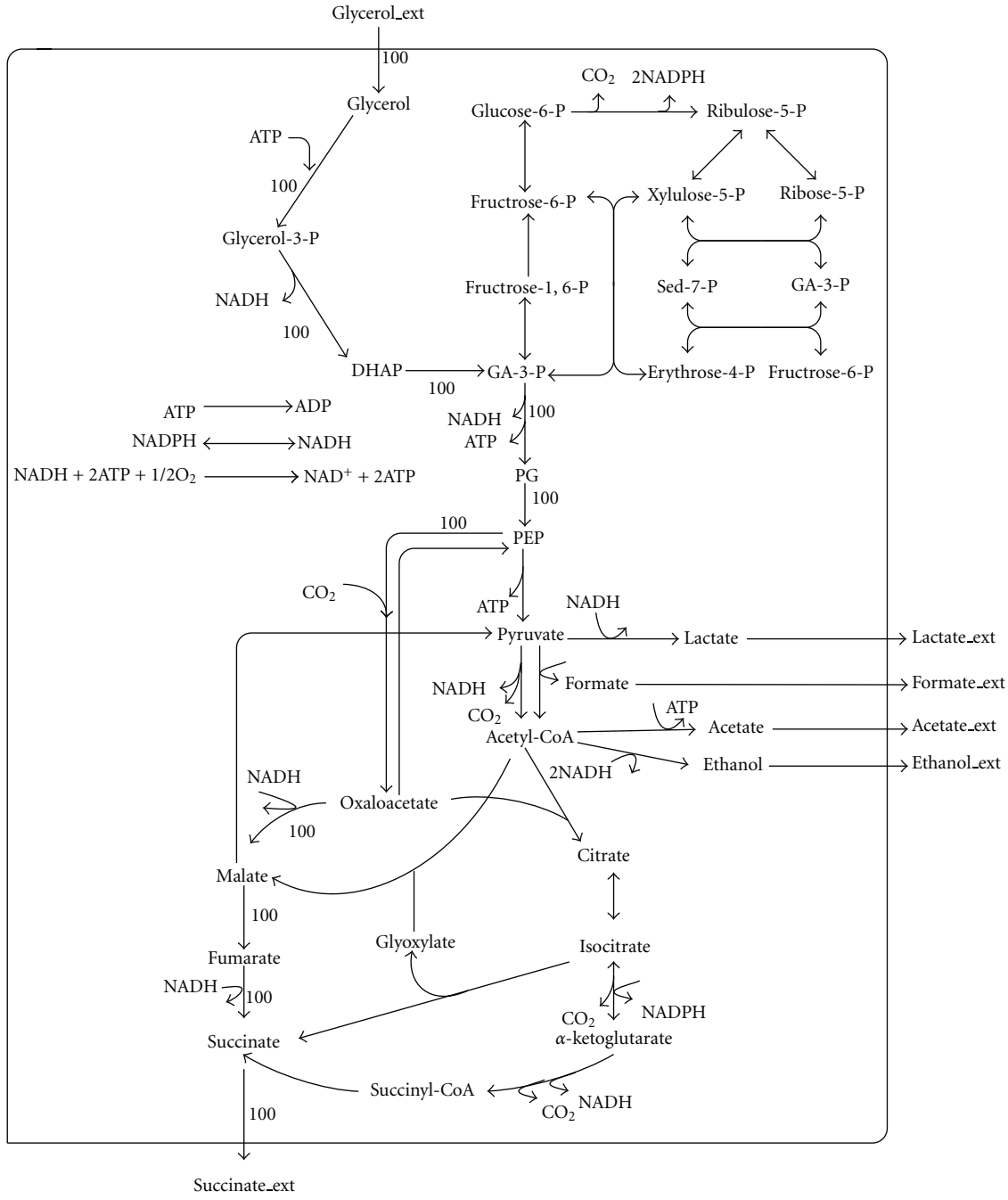

Figure 6: The optimum flux distribution of glycerol metabolism for succinate production in *E. coli* under aerobic conditions.

The influence of flux distribution at PEP node was shown in Figure 7(a). The succinate yield increased from 0.5 mol/mol to 1.0 mol/mol when R(40, 17) increased from 0 to 1.0. The results showed that increasing the flux distribution from PEP to oxaloacetate was beneficial for succinate production. For acetyl-CoA node, it was consumed in reactions R22, R44, R50, and R53 which are catalyzed by citrate synthase, aldehyde dehydrogenase, malate synthase, and phosphate acetyltransferase, respectively. The flux ratio was denoted as

$$\mathrm{R}(22, 44, 50, 53) = \frac{\mathrm{R22}}{(\mathrm{R22} + \mathrm{R44} + \mathrm{R50} + \mathrm{R53})}. \quad (4)$$

The influence of flux distribution at acetyl-CoA node was shown in Figure 7(b). The succinate yield decreased from 1.0 mol/mol to 0.75 mol/mol when R(22, 44, 50, 53) increased from 0 to 1.0. The results indicated that decreasing the flux distribution from acetyl to TCA cycle was beneficial for succinate production since the carbon would be lost during the TCA cycle.

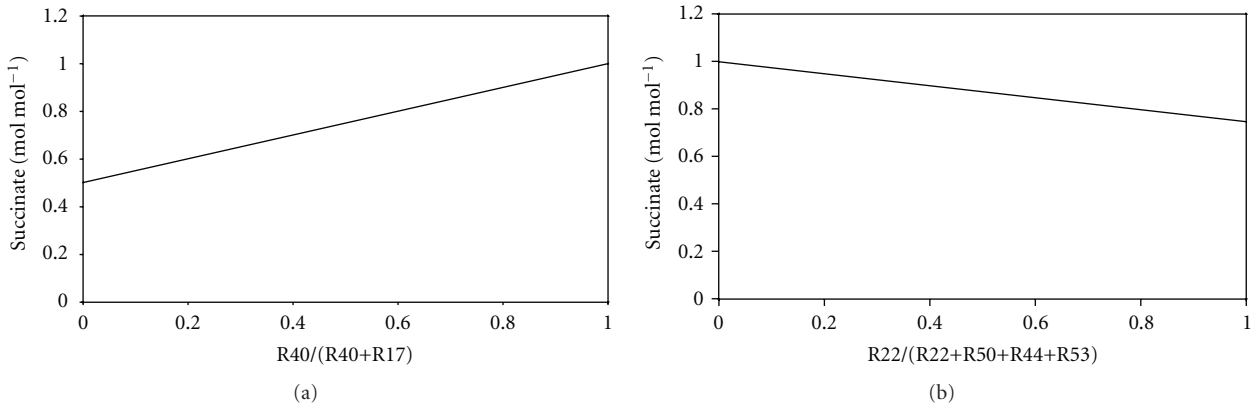

Figure 7: Sensitivity of succinate yield to the relative fluxes at the (a) PEP node and (b) AcCoA node under aerobic conditions. The PEP node involves the catabolic reactions of R40 and R17 which are catalyzed by PEP carboxylase and pyruvate kinase, respectively. The AcCoA node involves the catabolic reactions of R22, R50, R44, and R53 which are catalyzed by citrate synthase, aldehyde dehydrogenase, malate synthase, and phosphate acetyltransferase, respectively.

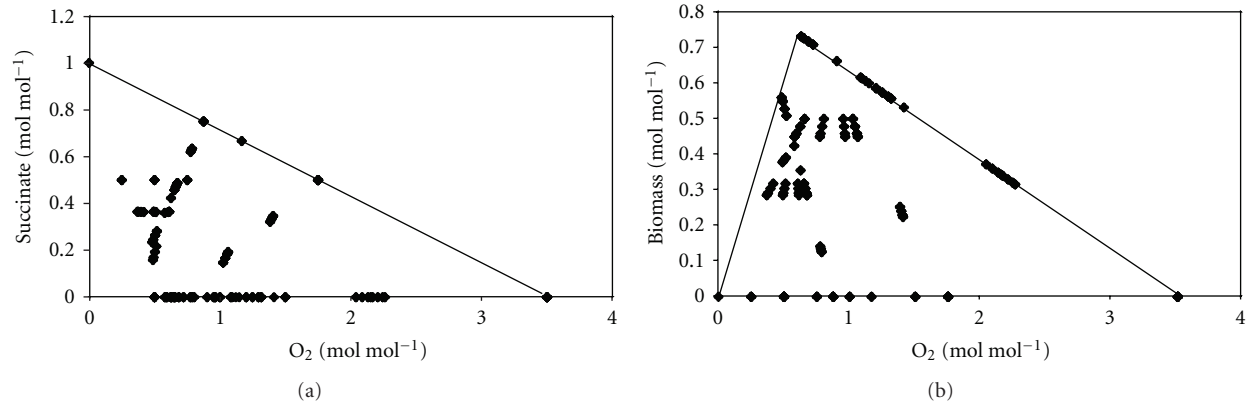

Figure 8: Effect of oxygen consumption on the succinate production and biomass formation under aerobic conditions. The enclosed regions represent the possible solution space. The fluxes were normalized by glycerol uptake rate and expressed as mol/mol (glycerol).

3.3. Effect of Oxygen Consumption on the Production of Succinate and Biomass. The effect of oxygen consumption on succinate and biomass production was further investigated according to the elementary mode analysis; the relationship between the molar fractions of oxygen consumption and succinate or biomass under aerobic conditions was calculated and shown in Figure 8. The theoretical succinate yield decreased as the oxygen consumption ratio increased (Figure 8(a)). The elementary modes of succinate yield distributed only on the left part of the solution space, which indicated that the higher consumption of oxygen was unfavorable for the succinate production. This is reasonable from the redox consideration. The higher consumption of oxygen results in more NAD which is critical for succinate production, to be utilized for the ATP production through oxidative phosphorylation. Especially as the molar oxygen consumption fraction of oxygen was more than 1.75 mol/mol, the elementary mode that produced succinate did not exist.

The theoretical biomass yield increased firstly and then decreased when the oxygen consumption ratio increased (Figure 8(b)). This is reasonable and consistent with the results of electron conservation because the rational increase of oxygen flux would be favorable for ATP synthesis through oxidative phosphorylation which is essential for biomass synthesis. However, high oxygen flux also results in less carbon source and reducing equivalents available for biomass because more carbon source would be oxidized to CO_2. The maximum biomass was achieved when the molar fraction of oxygen was 0.65 mol/mol. Since higher cell concentration is beneficial for increase of the productivity, the optimal regulation strategy is controlling the molar fraction of oxygen consumption less than 0.65 mol/mol.

3.4. Rational Design to Improve the Succinate Production by Genetic Modifications. Comparing the results of elementary flux mode analysis above, although the maximum succinate yields were 1.0 mol/mol under both anaerobic and aerobic

conditions, the aerobic condition seemed to be more favorable for succinate production in fact. The slow cell growth under anaerobic condition hindered the practical application of glycerol fermentation for succinate production [33]. What is more, the association of cell growth with the production of 1,2-propanediol, ethanol, and formate reduced the total yield of succinate.

As discussed above, to improve the yield of succinate yield under anaerobic condition, the substitution of PEP-dependent DHA kinase into ATP-dependent DHA kinase and overexpressing the PEP carboxylase would be a prior consideration. An alternative choice is to express the heterogeneous pyruvate carboxylase in *E. coli*. The overexpression of pyruvate carboxylase could redistribute the flux of pyruvate into oxaloacetate for succinate production. The optimal flux distribution for succinate production in such case could also reach 1.0 mol/mol which was shown in Figure 4. It has been reported that expressing the ATP-dependent DHA kinase and pyruvate carboxylase could both increase the yield of succinate [14]. Another consideration to increase the succinate yield is reducing the byproducts production. Since the production of 1,2-propanediol, ethanol, and formate is necessary for biomass synthesis, the proper strategy is reducing the acetate and lactate production. Knockout of the phosphate acetyltransferase gene (*pta*) and lactate dehydrogenase gene (*ldh*) would be expected to increase the succinate production.

For the case of aerobic condition, overexpressing the PEP carboxylase or expressing pyruvate carboxylase would be a prior consideration as discussed above. Knockdown of the isocitrate dehydrogenase gene (*icd*) would enhance the succinate production since the flux flowed from isocitrate to alpha-ketoglutarate and succinyl-CoA would result in the carbon lost. Since acetate is the main byproduct under aerobic condition [34], knocking out the pyruvate oxidase gene (*poxB*) and phosphate acetyltransferase gene (*pta*) is also expected to increase the succinate yield.

4. Conclusions

Nowadays, the conversion of byproduct glycerol has attracted more and more attention with the development of biodesiel industrial. The potentials of using glycerol for succinate production in *E. coli* under the anaerobic and aerobic conditions were compared by using elementary mode analysis in this work. The aerobic conditions seem to be more favorable for succinate production and the maximum succinate yield was 1.0 mol/mol. Although increase of the oxygen concentration would reduce the succinate yield, controlling the molar fraction of oxygen under 0.65 mol/mol would be beneficial for increasing the succinate productivity. According to the elementary mode analysis, the rational design was obtained for improving the succinate production by genetic modification under aerobic and anaerobic conditions, respectively. The results are considered useful for further investigation on the succinate metabolism of *E. coli*. The information also is beneficial for the efficient production of succinate from glycerol by *E. coli*.

Appendices

A. Models Used in This Study

A.1. Reactions and Enzymes Involved in Figure 1 (see Table 1).

A.2. The Anaerobic Metabolic Network Model Input File Used for the Program METATOOL.

(i) ENZREV (reversible reactions)

R10r R11r R14r R15r R16r R23r R26r R27r R28r R29r R31r R32r R33r R34r R35r R71r R86r.

(ii) ENZIRREV (irreversible reactions)

R1 R2 R3 R6 R7 R13 R17 R21 R22 R24 R30 R40 R41 R42 R43 R44 R50 R51 R53 R60 R70 R80 R81 R82 R83 R84 R85.

(iii) METINT (internal metabolite declaration)

Glycerol DHA DHAP GA-3-P propanediol PG PEP Pyruvate Acetyl-CoA CoASH Oxaloacetate Citrate Isocitrate a-Ketoglutarate Succinate Fumarate Malate Glyoxylate Glucose-6-P Fructrose-6-P Fructrose-16-P Ribulose-5-P Xylulose-5-P Ribose-5-P Sed-7-P Erythrose-4-P Lactate Formate Acetate Ethanol NAD NADH ATP ADP NADP NADPH CO_2.

(iv) METEXT (external metabolite declaration)

Glycerol_ext Ethanol_ext Acetate_ext CO_2_ext Lactate_ext Succinate_ext Formate_ext BIOMASS propanediol_ext.

(v) CAT

Reactions

(vi) Glycerol specific metabolisms

R1: Glycerol_ext = Glycerol.
R2: Glycerol + NAD = DHA + NADH.
R3: PEP + DHA = DHAP + Pyruvate.
R6: DHAP + 2NADH = propanediol + NAD.
R7: DHA + ATP = DHAP + ADP.

(vii) Glycolysis

R10r: DHAP = GA-3-P.
R11r: DHAP + GA-3-P = Fructrose-16-P.
R13: Fructrose-16-P = Fructrose-6-P.
R14r: Fructrose-6-P = Glucose-6-P.
R15r: GA-3-P + ADP + NAD = PG + ATP + NADH.
R16r: PG = PEP.
R17: PEP + ADP = PYR + ATP.

(viii) TCA cycle

R21: PYR + CoASH = Acetyl-CoA + FORMATE.
R22: Oxaloacetate + Acetyl-CoA = Citrate + CoASH.
R23r: Citrate = Isocitrate.

R24: Isocitrate + NADP = a-Ketoglutarate + NADPH + CO_2.
R27r: Succinate + NAD = Fumarate + NADH.
R28r: Fumarate = Malate.
R29r: Malate + NAD = Oxaloacetate + NADH.

(ix) Pentose Phosphate Pathway

R30: Glucose-6-P + 2NADP = Ribulose-5-P + 2NADPH + CO_2.
R31r: Ribulose-5-P = Xylulose-5-P.
R32r: Ribulose-5-P = Ribose_5_P.
R33r: Ribose-5-P + Xylulose-5-P = Sed-7-P + GA-3-P.
R34r: GA-3-P + Sed-7-P = Erythrose-4-P + Fructrose-6-P.
R35r: Erythrose-4-P + Xylulose-5-P = GA-3-P + Fructrose-6-P.

(x) Anapleurotic reactions

R40: PEP + CO_2 = Oxaloacetate.
R41: Oxaloacetate + ATP = PEP + ADP + CO_2 .
R42: MALATE + NADP = Pyruvate + NADPH + CO_2 .
R43: Isocitrate = Glyoxylate + Succinate.
R44: Glyoxylate + Acetyl-CoA = Malate + CoASH.

(xi) Redox-associated reactions

R50: Acetyl-CoA + 2NADH = Ethanol + 2NAD + CoASH.
R51: Pyruvate + NADH = Lactate + NAD.
R53: Acetyl-CoA + ADP = Acetate + CoASH + ATP.

(xii) Biomass formation

R60: 0.0206Glucose-6-P + 0.0072Fructrose-6-P + 0.0627Ribose-5-P + 0.0361 Erythrose-4-P + 0.0129GA-3-P + 0.1338PG + 0.0720PEP + 0.2861Pyruvate + 0.2930Acetyl-CoA + 0.1481 Oxaloacetate + 0.1078 a-Ketoglutarate + 1.6548 NADPH + 1.7821ATP + 0.3548 NAD = 2.87 BIOMASS + 1.6548 NADP + 0.2930 CoASH + 0.1678 CO_2 + 1.7821 ADP + 0.3548 NADH.

(xiii) Oxidative phosphorylation/maintenance energy

R70: ATP = ADP.
R71r: NADPH + NAD = NADH + NADP.

(xiv) Membrane transport reactions

R80: Lactate = Lactate_ext.
R81: Formate = Formate_ext.
R82: Acetate = Acetate_ext.
R83: Ethanol = Ethanol_ext.
R84: Succinate = Succinate_ext.
R85: propanediol = propanediol_ext.
R86r: CO_2 = CO_2_ext.

A.3. The Aerobic Metabolic Network Model Input File Used for the Program METATOOL.

(i) ENZREV (reversible reactions)

R10r R11r R14r R15r R16r R23r R26r R27r R28r R29r R31r R32r R33r R34r R35r R71r R86r.

(ii) ENZIRREV (irreversible reactions)

R1 R4 R5 R13 R17 R20 R22 R24 R25 R30 R40 R41 R42 R43 R44 R50 R51 R53 R60 R70 R72 R80 R81 R82 R83 R84 R87.

(iii) METINT (internal metabolite declaration)

Glycerol Glycerol-3-P DHAP GA-3-P PG PEP Pyruvate Acetyl-CoA CoASH Oxaloacetate Citrate Isocitrate a-Ketoglutarate Succinyl-CoA Succinate Fumarate Malate Glyoxylate Glucose-6-P Fructrose-6-P Fructrose-16-P Ribulose-5-P Xylulose-5-P Ribose-5-P Sed-7-P Erythrose-4-P Lactate Acetate Ethanol NAD NADH ATP ADP NADP NADPH CO_2 O_2.

(iv) METEXT (external metabolite declaration)

Glycerol_ext Ethanol_ext Acetate_ext CO_2_ext Lactate_ext Succinate_ext BIOMASS O_2_ext.

(v) CAT

Reactions

(vi) Glycerol specific metabolisms

R1: Glycerol_ext = Glycerol.
R4: Glycerol + ATP = Glycerol-3-P + ADP.
R5: Glycerol-3-P + NAD = DHAP + NADH.

(vii) Glycolysis

R10r: DHAP = GA-3-P.
R11r: DHAP + GA-3-P = Fructrose-16-P.
R13: Fructrose-16-P = Fructrose-6-P.
R14r: Fructrose-6-P = Glucose-6-P.
R15r: GA-3-P + ADP + NAD = PG + ATP + NADH.
R16r: PG = PEP.
R17: PEP + ADP = Pyruvate + ATP.

(viii) TCA cycle

R20: Pyruvate + CoASH + NAD = Acetyl-CoA + CO_2 + NADH.
R22: Oxaloacetate + Acetyl-CoA = Citrate + CoASH.
R23r: Citrate = Isocitrate.
R24: Isocitrate + NADP = a-Ketoglutarate + NADPH + CO_2.
R25: a-Ketoglutarate + NAD + CoASH = Succinyl-CoA + NADH + CO_2.
R26r: Succinyl-CoA + ADP = Succinate + ATP + CoASH.
R27r: Succinate + NAD = Fumarate + NADH.

R28r: Fumarate = Malate.
R29r: Malate + NAD = Oxaloacetate + NADH.

(ix) Pentose Phosphate Pathway

R30: Glucose-6-P + 2NADP = Ribulose-5-P + 2NADPH + CO_2.
R31r: Ribulose-5-P = Xylulose-5-P.
R32r: Ribulose-5-P = Ribose_5_P.
R33r: Ribose-5-P + Xylulose-5-P = Sed-7-P + GA-3-P.
R34r: GA-3-P + Sed-7-P = Erythrose-4-P + Fructrose-6-P.
R35r: Erythrose-4-P + Xylulose-5-P = GA-3-P + Fructrose-6-P.

(x) Anapleurotic reactions

R40: PEP + CO_2 = Oxaloacetate.
R41: Oxaloacetate + ATP = PEP + ADP + CO_2.
R42: MALATE + NADP = Pyruvate + NADPH + CO_2.
R43: Isocitrate = Glyoxylate + Succinate.
R44: Glyoxylate + Acetyl-CoA = Malate + CoASH.

(xi) Redox-associated reactions

R50: Acetyl-CoA + 2NADH = Ethanol + 2NAD + CoASH.
R51: Pyruvate + NADH = Lactate + NAD.
R52: Pyruvate = CO_2 + Acetate.
R53: Acetyl-CoA + ADP = Acetate + CoASH + ATP.

(xii) Biomass formation

R60: 0.0206Glucose-6-P + 0.0072Fructrose-6-P + 0.0627Ribose-5-P + 0.0361 Erythrose-4-P + + 0.0129GA-3-P + 0.1338PG + 0.0720PEP + 0.2861Pyruvate + 0.2930Acetyl-CoA + 0.1481 Oxaloacetate + 0.1078 a-Ketoglutarate + 1.6548 NADPH + 1.7821ATP + 0.3548 NAD = 2.87 BIOMASS + 1.6548 NADP + 0.2930 CoASH + 0.1678 CO_2 + 1.7821 ADP + 0.3548 NADH.

(xiii) Oxidative phosphorylation/maintenance energy:

R70: ATP = ADP.
R71r: NADPH + NAD = NADH + NADP.
R72: NADH + 2ADP + 1/2O_2 = NAD + 2ATP.

(xiv) Membrane transport reactions

R80: Lactate = Lactate_ext.
R82: Acetate = Acetate_ext.
R83: Ethanol = Ethanol_ext.
R84: Succinate = Succinate_ext.
R86r: CO_2 = CO_2_ext.
R87: O_2_ext = O_2.

A.4. Degree of Reduction of Considered Substrates and Products (see Table 2).

Nomenclature

Acetyl-CoA:	Acetyl-coenzyme A
ADP:	Adenosine diphosphate
ATP:	Adenosine triphosphate
DHA:	Dihydroxyacetone
DHAP:	Dihydroxyacetone phosphate
Erythrose-4-P:	Erythrose-4-phosphate
Fructose-6-P:	Fructose-6-phosphate
GA-3-P:	Glyceraldehyde-3-phosphate
Glucose-6-P:	Glucose-6-phosphate
NAD:	Nicotinamide adenine dinucleotide
NADH:	Nicotinamide adenine dinucleotide
1,2-PDO:	1,2-propanediol
PEP:	Phosphoenolpyruvate
PG:	Phosphoglycerate
Ribose-5-P:	Ribose-5-phosphate
Ribulose-5-P:	Ribulose-5-phosphate
Sed-7-P:	Sedoheptulose-7-P
Succinyl-CoA:	Succinyl-coenzyme A
Xylulose-5-P:	Xylulose-5-phosphate.

References

[1] S. S. Yazdani and R. Gonzalez, "Anaerobic fermentation of glycerol: a path to economic viability for the biofuels industry," *Current Opinion in Biotechnology*, vol. 18, no. 3, pp. 213–219, 2007.
[2] Y. Xu, H. Liu, W. Du, Y. Sun, X. Ou, and D. Liu, "Integrated production for biodiesel and 1,3-propanediol with lipase-catalyzed transesterification and fermentation," *Biotechnology Letters*, vol. 31, no. 9, pp. 1335–1341, 2009.
[3] Z. Chen, H. Liu, and D. Liu, "Regulation of 3-hydroxypropionaldehyde accumulation in Klebsiella pneumoniae by overexpression of dhaT and dhaD genes," *Enzyme and Microbial Technology*, vol. 45, no. 4, pp. 305–309, 2009.
[4] Z. Chen, H.-J. Liu, J.-A. Zhang, and D.-H. Liu, "Cell physiology and metabolic flux response of Klebsiella pneumoniae to aerobic conditions," *Process Biochemistry*, vol. 44, no. 8, pp. 862–868, 2009.
[5] S. Shams Yazdani and R. Gonzalez, "Engineering Escherichia coli for the efficient conversion of glycerol to ethanol and co-products," *Metabolic Engineering*, vol. 10, no. 6, pp. 340–351, 2008.
[6] D. Rittmann, S. N. Lindner, and V. F. Wendisch, "Engineering of a glycerol utilization pathway for amino acid production by Corynebacterium glutamicum," *Applied and Environmental Microbiology*, vol. 74, no. 20, pp. 6216–6222, 2008.
[7] I. R. Booth, "Glycerol and methylglyoxal metabolism," in *EcoSal—Escherichia coli and Salmonella: Cellular and Molecular Biology*, R. Curtis III, et al., Ed., ASM Press, Washington, DC, USA, 2005.
[8] Y. D. Kwon, S. Y. Lee, and P. Kim, "Influence of gluconeogenic phosphoenolpyruvate carboxykinase (PCK) expression on succinic acid fermentation in Escherichia coli under high bicarbonate condition," *Journal of Microbiology and Biotechnology*, vol. 16, no. 9, pp. 1448–1452, 2006.

[9] H. Lin, K.-Y. San, and G. N. Bennett, "Effect of Sorghum vulgare phosphoenolpyruvate carboxylase and Lactococcus lactis pyruvate carboxylase coexpression on succinate production in mutant strains of Escherichia coli," *Applied Microbiology and Biotechnology*, vol. 67, no. 4, pp. 515–523, 2005.

[10] S. H. Hong and S. Y. Lee, "Metabolic flux analysis for succinic acid production by recombinant Escherichia coli with amplified malic enzyme activity," *Biotechnology and Bioengineering*, vol. 74, no. 2, pp. 89–95, 2001.

[11] W. B. Freedberg and E. C. C. Lin, "Three kinds of controls affecting the expression of the glp regulon in Escherichia coli," *Journal of Bacteriology*, vol. 115, no. 3, pp. 816–823, 1973.

[12] G. Sweet, C. Gandor, R. Voegele et al., "Glycerol facilitator of Escherichia coli: cloning of glpF and identification of the glpF product," *Journal of Bacteriology*, vol. 172, no. 1, pp. 424–430, 1990.

[13] Y. Dharmadi, A. Murarka, and R. Gonzalez, "Anaerobic fermentation of glycerol by Escherichia coli: a new platform for metabolic engineering," *Biotechnology and Bioengineering*, vol. 94, no. 5, pp. 821–829, 2006.

[14] A. Murarka, Y. Dharmadi, S. S. Yazdani, and R. Gonzalez, "Fermentative utilization of glycerol by Escherichia coli and its implications for the production of fuels and chemicals," *Applied and Environmental Microbiology*, vol. 74, no. 4, pp. 1124–1135, 2008.

[15] N. E. Altaras and D. C. Cameron, "Metabolic engineering of a 1,2-propanediol pathway in Escherichia coli," *Applied and Environmental Microbiology*, vol. 65, no. 3, pp. 1180–1185, 1999.

[16] J. A. Papin, J. Stelling, N. D. Price, S. Klamt, S. Schuster, and B. O. Palsson, "Comparison of network-based pathway analysis methods," *Trends in Biotechnology*, vol. 22, no. 8, pp. 400–405, 2004.

[17] C. H. Schilling, D. Letscher, and B. O. Palsson, "Theory for the systemic definition of metabolic pathways and their use in interpreting metabolic function from a pathway-oriented perspective," *Journal of Theoretical Biology*, vol. 203, no. 3, pp. 229–248, 2000.

[18] S. Schuster, T. Dandekar, and D. A. Fell, "Detection of elementary flux modes in biochemical networks: a promising tool for pathway analysis and metabolic engineering," *Trends in Biotechnology*, vol. 17, no. 2, pp. 53–60, 1999.

[19] J. O. Krömer, C. Wittmann, H. Schröder, and E. Heinzle, "Metabolic pathway analysis for rational design of L-methionine production by Escherichia coli and Corynebacterium glutamicum," *Metabolic Engineering*, vol. 8, no. 4, pp. 353–369, 2006.

[20] R. Carlson, D. Fell, and F. Srienc, "Metabolic pathway analysis of a recombinant yeast for rational strain development," *Biotechnology and Bioengineering*, vol. 79, no. 2, pp. 121–134, 2002.

[21] N. C. Duarte, B. ∅. Palsson, and P. Fu, "Integrated analysis of metabolic phenotypes in Saccharomyces cerevisiae," *BMC Genomics*, vol. 5, article 63, 2004.

[22] J. C. Liao and M.-K. Oh, "Toward predicting metabolic fluxes in metabolically engineered strains," *Metabolic Engineering*, vol. 1, no. 3, pp. 214–223, 1999.

[23] R. Carlson and F. Srienc, "Fundamental Escherichia coli biochemical pathways for biomass and energy production: creation of overall flux states," *Biotechnology and Bioengineering*, vol. 86, no. 2, pp. 149–162, 2004.

[24] N. Vijayasankaran, R. Carlson, and F. Srienc, "Metabolic pathway structures for recombinant protein synthesis in Escherichia coli," *Applied Microbiology and Biotechnology*, vol. 68, no. 6, pp. 737–746, 2005.

[25] Q. Zhang and Z. Xiu, "Metabolic pathway analysis of glycerol metabolism in Klebsiella pneumoniae incorporating oxygen regulatory system," *Biotechnology Progress*, vol. 25, no. 1, pp. 103–115, 2009.

[26] U. Sauer, F. Canonaco, S. Heri, A. Perrenoud, and E. Fischer, "The soluble and membrane-bound transhydrogenases UdhA and PntAB have divergent functions in NADPH metabolism of Escherichia coli," *Journal of Biological Chemistry*, vol. 279, no. 8, pp. 6613–6619, 2004.

[27] R. Carlson and F. Srienc, "Fundamental Escherichia coli biochemical pathways for biomass and energy production: identification of reactions," *Biotechnology and Bioengineering*, vol. 85, no. 1, pp. 1–19, 2004.

[28] J. S. Edwards and B. O. Palsson, "Metabolic flux balance analysis and the in silico analysis of Escherichia coli K-12 gene deletions," *BMC Bioinformatics*, vol. 1, article 1, 2000.

[29] A. Hasona, Y. Kim, F. G. Healy, L. O. Ingram, and K. T. Shanmugam, "Pyruvate formate lyase and acetate kinase are essential for anaerobic growth of Escherichia coli on xylose," *Journal of Bacteriology*, vol. 186, no. 22, pp. 7593–7600, 2004.

[30] J. M. Berg, J. L. Tymoczko, and L. Stryer, *Biochemistry*, WH Freeman, 5th edition, 2002.

[31] A. von Kamp and S. Schuster, "Metatool 5.0: fast and flexible elementary modes analysis," *Bioinformatics*, vol. 22, no. 15, pp. 1930–1931, 2006.

[32] T. Pfeiffer, I. Sánchez-Valdenebro, J. C. Nuño, F. Montero, and S. Schuster, "METATOOL: for studying metabolic networks," *Bioinformatics*, vol. 15, no. 3, pp. 251–257, 1999.

[33] C. T. Trinh and F. Srienc, "Metabolic engineering of Escherichia coli for efficient conversion of glycerol to ethanol," *Applied and Environmental Microbiology*, vol. 75, no. 21, pp. 6696–6705, 2009.

[34] H. Lin, G. N. Bennett, and K.-Y. San, "Metabolic engineering of aerobic succinate production systems in Escherichia coli to improve process productivity and achieve the maximum theoretical succinate yield," *Metabolic Engineering*, vol. 7, no. 2, pp. 116–127, 2005.